Neuronal circuits overcome imbalance in excitation and inhibition by adjusting connection numbers

Nirit Sukenik[a,1], Oleg Vinogradov[b,c,d,1] (ID), Eyal Weinreb[a] (ID), Menahem Segal[e,2] (ID), Anna Levina[b,d,2,3] (ID), and Elisha Moses[a,2,3]

[a]Department of Physics of Complex Systems, Weizmann Institute of Science, Rehovot 7610001, Israel; [b]Department of Computer Science, University of Tübingen, 72076 Tübingen, Germany; [c]Graduate Training Centre of Neuroscience, University of Tübingen, 72074 Tübingen, Germany; [d]Max Planck Institute for Biological Cybernetics, 72076 Tübingen, Germany; and [e]Department of Neurobiology, Weizmann Institute of Science, Rehovot 7610001, Israel

The interplay between excitation and inhibition is crucial for neuronal circuitry in the brain. Inhibitory cell fractions in the neocortex and hippocampus are typically maintained at 15 to 30%, which is assumed to be important for stable dynamics. We have studied systematically the role of precisely controlled excitatory/inhibitory (E/I) cellular ratios on network activity using mice hippocampal cultures. Surprisingly, networks with varying E/I ratios maintain stable bursting dynamics. Interburst intervals remain constant for most ratios, except in the extremes of 0 to 10% and 90 to 100% inhibitory cells. Single-cell recordings and modeling suggest that networks adapt to chronic alterations of E/I compositions by balancing E/I connectivity. Gradual blockade of inhibition substantiates the agreement between the model and experiment and defines its limits. Combining measurements of population and single-cell activity with theoretical modeling, we provide a clearer picture of how E/I balance is preserved and where it fails in living neuronal networks.

E/I balance | neuronal network | network dynamics | bursting

Neuronal circuits in the brain are composed of a combination of excitatory and inhibitory neurons. While the role of excitatory cells is directly related to the spreading of network activity in and outside of these networks, the inhibitory neurons provide recurrent feedback regulation of the activity. Clearly, a circuit will need the negative feedback realized by the inhibitory population to function in a complementary and coordinated relation with the excitatory cells. The balance of these two opposing forces is the focus of most network models comprised of both neuron types. However, a definite quantitative resolution of how the excitation/inhibition (E/I) balance is maintained has not yet been formulated.

The E/I ratio has been shown to control many aspects of the activity of large-scale neural networks. For instance, experimental studies show that precise coordination of excitatory and inhibitory inputs shape the activity of populations of neurons in sensory cortices (1, 2). At the same time, the interplay of excitation and inhibition is often proposed as a fundamental mechanism for generating oscillations in the brain (1). Theoretical work has shown that changing the overall E/I ratio plays a major role in controlling dynamic states, stability, and coding capabilities of neuronal networks, with the resulting network activity ranging from asynchronous, irregular firing to synchronized network bursting (3, 4).

Inhibition in the cortical areas is implemented by GABAergic neurons, which comprise about 20 to 30% of all cortical neurons. This proportion is conserved across mammalian species and during the lifespan of an animal (5). The importance of keeping a specific fixed inhibitory percentage has been postulated to be linked to efficient storage capacity (6) and to multitask learning (7), among many other functions related to the hippocampus. However, the importance of having this particular fraction of inhibitory neurons for the general control of network dynamics remains unclear.

Another well-studied aspect of cortical organization is that excitation and inhibition are balanced both structurally and dynamically. Dynamically, excitatory, and inhibitory inputs strongly correlate and

synchronize in both spontaneous and evoked activity (2, 8, 9). Structurally, the ratio of excitatory and inhibitory synapses converging onto one cell is approximately constant (8), but the location of the synapses determines the efficacy of network firing. Inhibitory synapses can be located on remote or proximal dendrites, as well as on the axon initial segment, where they block the ability of the neuron to discharge action potentials. The role of inhibition is further complicated by the fact that there are several types of inhibitory neurons that can be clustered by their locus of action on the excitatory neurons as well as the formation of inhibitory synapses on interneurons (10). For the sake of simplicity, we will not discuss in the present study the role of different types of interneurons on network activity.

Perturbations of the E/I ratio that move the network away from its balance have been reported recently and can be applied both acutely and chronically. Acute blockade of inhibitory synapses in vitro by application of pharmacological agents causes the dynamics to be excitatory dominated, more uniform, and synchronized (11, 12). Blocking inhibition acutely in vivo has been found to create epileptic seizures (13). In contrast, chronic blockade (about 48 h) or overactivation of inhibition causes neuronal networks to adjust their activity (8). Changes in the E/I balance have been linked to different brain states like deep anesthesia (14). Furthermore, shifts in E/I balance were found to have far-reaching behavioral effects in freely moving mice (15).

Significance

Standard hippocampal circuitry contains about 20 to 30% inhibitory neurons. We show that cultured hippocampal networks maintain stable and robust dynamics in a wide range of precisely controlled cellular excitatory/inhibitory ratios. To uncover the mechanism underlying the stability of network dynamics, we use single-cell patch-clamp recordings. We suggest that the networks adapt to altered excitation/inhibition compositions by adjusting the number of connections. Our modeling of the collective dynamics observed experimentally demonstrates that neuronal networks self-organize toward excitation/inhibition balance via changes in connectivity.

NEUROSCIENCE

BIOPHYSICS AND COMPUTATIONAL BIOLOGY

Given that the conservation of E/I balance is a basic property of large-scale neuronal networks, it is pertinent to ask what mechanisms contribute to the creation of this balance and where their limitations become apparent. E/I balance was extensively studied in brain areas with 20 to 40% inhibitory cells (2, 16); however, there is no systematic view of how the inhibitory cell fraction and balance are related. To address this, we have engineered cultures of hippocampal neurons with precisely controlled numbers of excitatory and inhibitory cells over a wide range of E/I ratios from 0% inhibitory neurons to 100%. Our design imposes a global and chronic change to which the network must respond. We have asked whether, given enough time to adapt and rewire, a neuronal network can compensate for the perturbation and reach balanced and stable dynamics.

In the present study, we focus on the ability of neuronal networks with artificially obtained E/I ratios to adapt during their development in vitro by monitoring both the whole network dynamics and the single cell behavior. In parallel, we employ finite network models to directly relate the network properties with the collective dynamics. This enables the emergence of a unified picture of the accommodation to changing E/I ratios in the ensemble of active neurons.

Results

Fluorescence-Activated Cell Sorted Cultures Exhibit Collective Dynamics.
When dissociated neurons grow in culture, they evolve into a highly connected network that generates synchronized bursting activity separated by quiet periods. This activity emerges during the development of a network and is controlled by the architecture of its excitatory and inhibitory cells (17) and by the balance between them. To study the role of inhibitory cells in balancing and regulating network dynamics and connectivity, we change the fraction of inhibitory cells between 0 and 100% while keeping identical seeding densities (Fig. 1 and *SI Appendix, SI Methods*) and measure whole network spontaneous activity by fluorescent imaging. The experiments are done on cultures 14 to 30 d in vitro after the GABA switch had already occurred (18). This ensures that GABAergic cells had already acquired their inhibitory behavior. Examples for single pyramidal and GABAergic neurons observed in our matured cultures are shown in Fig. 2. We find that the final cellular density, after growing in vitro, is independent of inhibitory percentage with a mean $\pm$ SD value of 950 ± 130 cells/mm^2. We have further verified that network activity features presented in the result section do not depend on the density (*SI Appendix*, Table S2).

All cultures, with varying amounts of inhibitory cells, are spontaneously active and develop network bursting (Fig. 2*A*). For cultures with very high inhibitory percentage (Fig. 2*A*,
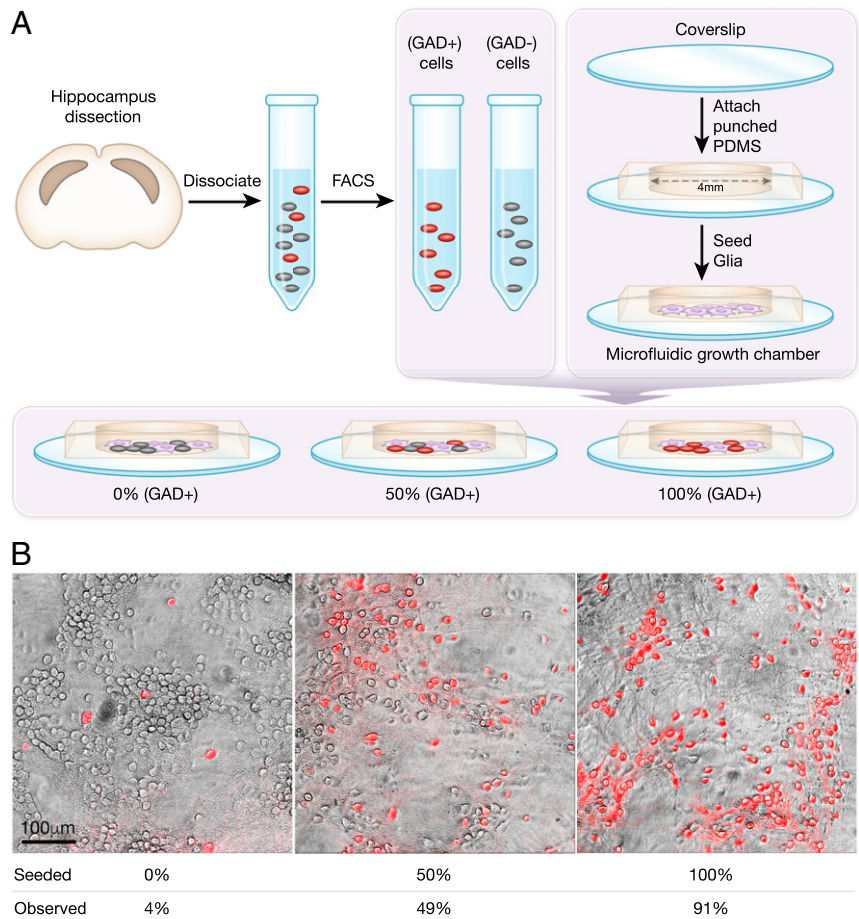

Fig. 1. Methods for culturing hippocampal networks with different E/I cellular compositions. (*A*) Hippocampal neurons are dissected from mouse embryos at day 17 of gestation. Females from mouse model GAD II-IRES-Cre are mated with males from mouse model Ai9-tdTomato-lox, yielding GABAergic cells that coexpress tdTomato with GAD II. FACS is used to sort tdTomato-expressing cells (GAD+ population, GABAergic cells) from those not expressing (GAD−). GAD+ and GAD− populations are then seeded at different ratios in microfluidic growth chambers on a glial cell layer. (*B*) Examples for three different cultures with seeding percentages of 0, 50, and 100% GABAergic cells and corresponding experimentally observed percentages of 4, 49, and 91%. Imaging was performed on a SP5 Leica confocal microscope with the fluorescent measurement overlaid on a transmitted light image.
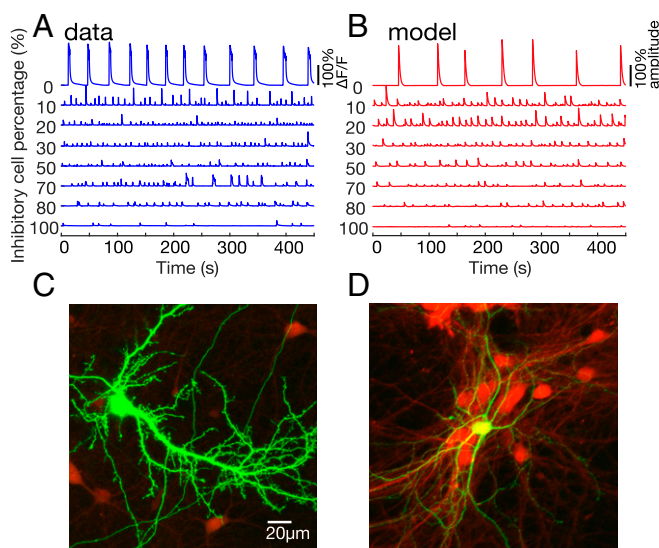
Fig. 2. Experiment and model bursting activity, along with neuron images. (*A*) Typical calcium imaging traces of the experimental data, displaying the percent deviation from baseline fluorescence ΔF/F. All cultures are spontaneously active, even at high inhibitory percentages. The control cultures (i.e., no sorting) are set as 25% inhibition. (*B*) The model simulations of networks with the inhibitory fractions that are used experimentally. The two model parameters are the number of inhibitory connections and the external input rate, sampled from the approximated posterior distribution (*SI Appendix, SI Methods*). To mimic the slow dynamics of the calcium indicator, network spike counts are convolved with a 2-s exponential kernel, and a sigmoid cutoff is applied on the amplitude. The amplitudes are normalized by the maximum amplitude of the 10% inhibitory network. The model agrees considerably with the experimental results. (*C* and *D*) Green fluorescent protein–transfected neurons (green) on background of tdTomato-cultured hippocampal neurons (red). A green pyramidal neuron is presented in *C*. The yellow (green+red) GABAergic neuron is shown in *D*; note that the dendrites of the GABAergic neuron are thin, the cell is multipolar, and there are no apparent dendritic spines. The green pyramidal cell has an apparent apical dendrite and many dendritic spines, indicating a genuine excitatory neuron.

bottom trace), this is an unexpected result since striatal cultures with ~95% inhibitory cells are reported not to exhibit synchronized spontaneous bursting (19). Cultures with 0% inhibitory cells (Fig. 2*A*, top trace) have significantly higher burst amplitudes than cultures with 20 to 100% inhibition, with up to a 10-fold difference. This effect is similar and even larger than that produced by acute blockade of inhibition, which typically causes a two to fivefold increase in amplitude (12).

Effect of E/I Composition on Network Dynamics. Features of bursting activity are a good indicator for the structure and connectivity of neuronal networks since they depend on the strength and amount of neuronal connections, as well as the ability of a network to recruit, recover, and propagate signals (17). Bursting dynamics of cultures are characterized by three main parameters: interburst intervals (IBI), burst amplitudes, and burst durations (*SI Appendix, SI Methods*).

IBIs are defined as the time between the initiations of two consecutive bursts. In Fig. 3 we present the major features of the spontaneous bursting, averaged over time per culture and then averaged over a set of cultures for each seeded inhibitory percentage. The numbers of cultures included in the analysis are as follows: n (0%) = 15, n (10%) = 12, n (20%) = 9, n (30%) = 11, n (50%) = 10, n (70%) = 13, n (80%) = 11, n (100%) = 13, n (25%/Control with no fluorescence-activated cell sorting [FACS]) = 9, obtained from between four and eight dissections. The mean of

the IBIs as a function of inhibitory cell percentage follows a U-shaped trend (Fig. 3*A*), remaining similar for most E/I ratios, except in extreme inhibitory percentages. In cultures with 10 to 80% inhibitory cells, the mean IBI values range between 10 ± 1 s (mean ± SEM) to 21 ± 6 s, whereas cultures with 0 and 100% seeded inhibitory percentages are characterized by significantly higher IBI values of 65 ± 5 s and 70 ± 19 s, respectively ($P < 0.0001$, permutation ANOVA). A small positive trend of the IBIs' mean is observed in 10 to 80% inhibitory cultures ($P = 0.039$). In contrast, the variability of the IBIs, measured by the coefficient of variation (CV), grows linearly with inhibitory percentage from 0.29 ± 0.03 to 0.75 ± 0.04 ($P = 5.4 \times 10^{-13}$, Fig. 3*B*). This suggests that as the number of inhibitory cells increases, the network proportionally adjusts itself to maintain stable dynamics, a process that introduces increasing variability to the system.

Burst amplitudes are an important feature that describe the bursting dynamics of a developing neuronal network (17), a process which correlates with the rate of generated spikes (20). A small increment of inhibitory neuron percentage, from almost no inhibition to 10% inhibition (Fig. 3*C*), leads to a fivefold drop in burst amplitudes from 1.4 ± 0.1 ΔF/F to 0.25 ± 0.03 ΔF/F (permutation ANOVA, $P < 0.001$). This behavior has a remarkable similarity to the effect of inhibition blockade (12). The amplitudes'
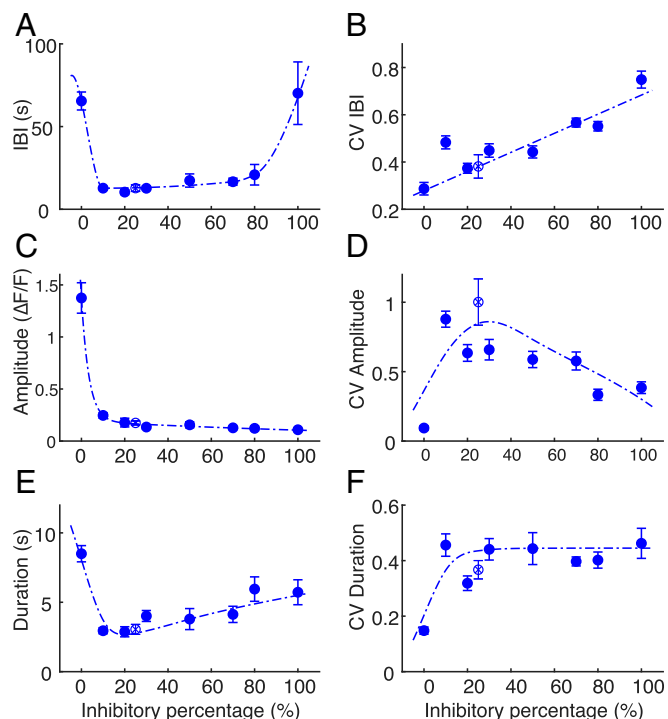

Fig. 3. Bursting dynamics as a function of E/I composition. (*A*) IBIs follow a U-shaped trend as function of inhibitory percentage, with higher values at the extreme cases (0 and 100%) but are relatively constant in midrange (10 to 80%). (*B*) The CV of IBIs, a measure of the variability, grows linearly along the full range of inhibitory percentages. (*C*) Burst amplitudes drop from 0 to 10% inhibition and continue to decay till 100% inhibition. (*D*) The CV of burst amplitude is minimal for 0% inhibition (0.09 ± 0.02). Increasing the inhibitory percentage to 10% leads to a sharp increase of amplitude variance, which then gradually decays at higher inhibition fractions. (*E*) Burst duration is maximal for 0% inhibition (8.5 ± 0.6 s) and abruptly decreases at 10% inhibition. The duration gradually increases with higher inhibitory percentage. (*F*) Durations of 0% inhibitory cultures exhibit a relatively low CV of 0.15 ± 0.01. Other fractions in the range of 10 to 100% inhibition display a relatively constant value around 0.45. In all panels, the dashed lines are meant only as a guide to the eye, the error bars indicate the SEM, and control (no FACS) is displayed as an empty circle with × inside.

CV (Fig. 3D) increases almost 10-fold (from 0.09 ± 0.02 to 0.88 ± 0.06) when the inhibitory percentage changes from 0 to 10%. In 0% and 50 to 100% cultures, the amplitudes' CVs are significantly smaller compared to control ($P = 0.0173$, $P = 0.0098$, $P < 0.0001$, and $P = 0.0002$) and were not significantly different in 10 to 30% cultures.

Burst durations (Fig. 3E) are the largest in 0% inhibitory cultures (8.5 ± 0.6 s), an effect that is comparable to that of blockade of inhibition, which broadens network bursts in cultured multi-electrode arrays (11). Burst durations in 0 and 80% cultures are significantly larger than in control cultures ($P < 0.05$). We also observe a positive trend in burst durations between 10 and 100% of inhibitory neurons ($P = 0.001$). Burst durations' CV rises from 0.15 ± 0.01 to 0.46 ± 0.04 between 0 and 10% ($P < 0.0001$) and stays approximately constant for 10 to 100% of inhibitory neurons (Fig. 3F).

Generally, bursting features of cultures with varying E/I ratios do not change considerably except for the extreme cases of 0 and 100%, and the dynamics are kept stable. Even a small inhibitory population suffices to effectively produce dynamics that are similar to those of control networks. We have verified that changes in burst amplitudes and in IBI do not originate in corresponding changes in levels of synchrony, which exhibits some interesting variation but remains high in all inhibitory percentages (*SI Appendix*, Figs. S4 and S5). We proceed and turn to single-neuron synaptic measurements in order to provide a possible mechanism for this stability.

The Number of Active Incoming Connections Decreases with Increasing Fraction of Inhibitory Cells. While the burst dynamics have proven effective in identifying the robustness of the network behavior under varying E/I ratios, uncovering the mechanism underlying this behavior requires single-neuron information. We establish this using patch-clamp measurements of both excitatory and inhibitory neurons. As shown in *SI Appendix*, we are able to clearly distinguish the excitatory from inhibitory neurons based on their electrophysiological properties (*SI Appendix*, Fig. S3).

Most modeling approaches regard the synaptic strength as determined by the size of the mean postsynaptic current (PSC). In Fig. 4, we present spontaneous PSCs as measured for three representative E/I ratios of 20, 50, and 80% inhibitory neurons. We measure this for 60 to 120 s while the network is between bursts. The numbers of excitatory cells measured for each fraction are $n = 12$ for 20%, $n = 7$ for 50%, and $n = 7$ for 80%, and the numbers of inhibitory cells are $n = 10$ for 20%, $n = 12$ for 50%, and $n = 22$ for 80%. Within our experimental errors, there is no statistically significant change in the size of PSCs ($P = 0.98$) for either the excitatory or the inhibitory cells as a function of the E/I ratio, as shown in Fig. 4 A, *Left*. Similarly, the decay time of PSCs remains unchanged for both excitatory and inhibitory neurons (Fig. 4 A, *Middle*, $P = 0.786$).

The size of the PSC is determined by the number of synapses that connect from a presynaptic cell to the postsynaptic cell, along with the strength of each synapse. Since the PSC amplitude does not vary much as compared to the rate, the simplest assumption is that both synapse number and strength remain unchanged (although in principle, both could change if these changes were somehow cancelling each other).

A dramatic change is observed in the frequency of PSCs as a function of E/I ratios, as shown in Fig. 4 A, *Right*, $P = 0.003$. Since the timing between two consecutive PSCs is relatively long, we can assume that they do not originate from the same action potential that reaches the terminals. The observed decrease in PSCs with E/I ratio is linear, and is consistent, within statistical error, with a direct proportionality to the number of excitatory cells (Fig. 4 A, *Right* and the associated *Inset*). The number of inputs to both inhibitory and excitatory neurons is thus directly proportional to the number of excitatory neurons.

In principle, the change in frequency of PSCs may be the result of a change in the firing rate of the presynaptic cell rather than a change in the number of incoming connections from neighboring neurons. To control for this possibility, we record miniature excitatory postsynaptic currents (mEPSCs) in the presence of tetrodotoxin (TTX) and bicuculline in both GABAergic and non-GABAergic neurons (Fig. 4 B and C). Since network activity is blocked under these conditions, any change in frequency will reflect a change in the number of presynaptic terminals connecting to the postsynaptic cell. Indeed, we find changes between cultures with 20 and 80% GABAergic neurons concurring with those seen without TTX (Fig. 4C).

This indicates that the number of presynaptic terminals connecting to the postsynaptic neuron has changed and suggests that connectivity, rather than adjustment of synaptic strength, drives the network response.

We also observe a strong difference in the PSC frequency of inhibitory versus excitatory neurons by about a factor of 7 ($P = 8.56 \times 10^{-11}$). This was seen both with and without TTX (Fig. 4 A
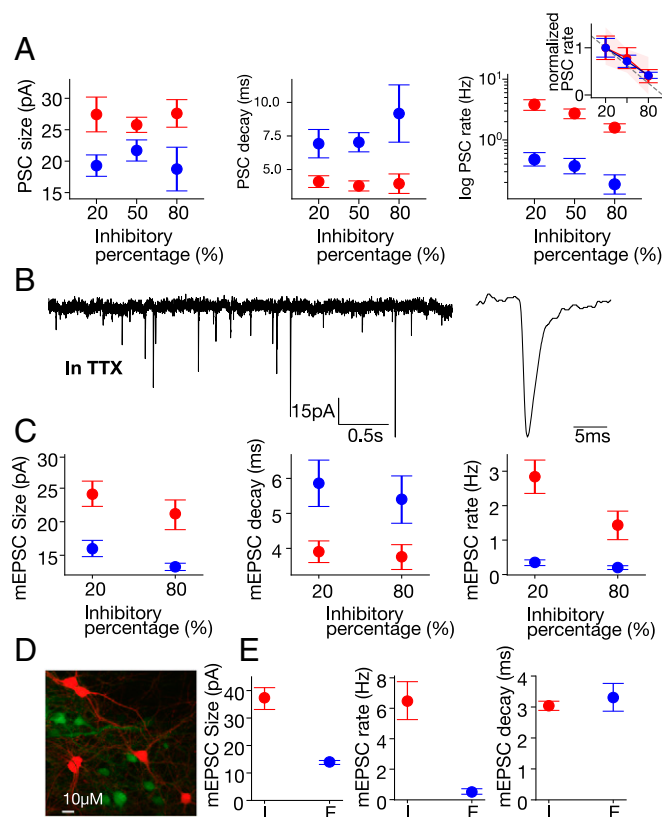

Fig. 4. Patch-clamp measurement. Single-cell changes (mean ± SEM) in response to varying the network inhibitory percentages is presented for inhibitory (red) and excitatory (blue) neurons. (A) While the size (*Left*) and decay time (*Middle*) of spontaneous PSCs do not change with inhibition, a significant decrease occurs in the PSC rate (*Right*, logarithmic scale). (*Inset*) Normalizing PSC rates by the value at 20% inhibition highlights the substantial (and similar) decrease for both excitatory and inhibitory cells. Moreover, the linear fit to the decrease (dashed line, 95% CI-red area) shows the rate to be directly proportional to the number of excitatory cells. (B) Sample mEPSCs (*Left*), recorded in 0.5 μM TTX and 10 μM bicuculline, from a red (inhibitory) cell in a 20% inhibitory culture (zoom-in, *Right*). (C) mEPSC size (*Left*) and decay time (*Middle*) also do not change with inhibition. However, the rate does change significantly, showing lower values at higher inhibition percentage (*Right*). (D) Image of a field containing red (CRE-GAD-tdTomato) and green (CRE-OFF-YFP) neurons. (E) Within the same culture, mEPSC size (*Left*) and rate (*Middle*) are significantly higher in inhibitory (I) versus excitatory (E) neurons, while the decay time (*Right*) is similar. See *SI Appendix, SI Methods* for the statistical analysis.

and *C*, respectively). To ensure that the actual fluorescence itself does not change the properties of neurons, we conduct experiments where we compare tdTomato CRE-GAD neurons with YFP CRE-OFF (virally)–stained neurons (Fig. 4*D*). These experiments show that the fluorescence of the cells in our system does not determine their behavior (Fig. 4*E*), maintaining the same mEPSC properties with and without viral transfection (Fig. 4 *C* and *E*).

A Network of Adaptive Leaky Integrate-and-Fire Neurons Can Reproduce the Main Features of the Dynamics. To relate dynamics with network properties, we have constructed a minimal interpretable network model that exhibits a bursting behavior. As shown in Fig. 5*A*, the network is composed of excitatory and inhibitory leaky integrate-and-fire (LIF) neurons with spike-triggered adaptation. Each neuron receives K^E excitatory and K^I inhibitory connections with synaptic strengths gJ and J, respectively, where g is a proportionality constant. The synaptic strength approximates the "functional synapse" with multiple axon collaterals. For this approximate model, the number of input connections at a given E/I ratio is the same (i.e., $K^E + K^I$ as the excitatory (blue) and inhibitory (red) neurons (Fig. 5*A*). All neurons, both inhibitory and excitatory, are additionally driven by an external Poisson input that models various sources of spontaneous activations of single neurons (*SI Appendix, SI Methods*). Assigning the same number of input connections (K^E and K^I) to both types of neurons is a simplification that disregards the experimentally observed sevenfold difference in PSC frequencies between excitatory and inhibitory neurons at the E/I ratios we have measured. We justify this simplification by the fact that this difference does not depend on the inhibitory fraction, expanding the model to precisely matched topologies remains a question for the follow-up studies. The model exhibits diverse network bursting that can be controlled by the synaptic strength, network connectivity, rate of external inputs, and the strength of adaptation (21, 22). Note

that the model is limited to reconstruct only the bursting dynamics on the level of spiking activity and does not fit the voltages of individual neurons during bursting (*SI Appendix*, Fig. S8).

Since the PSC amplitudes did not vary significantly across cultures with different fractions of inhibitory neurons, we fix the inhibitory and excitatory synaptic strength and do not explore its effects of on the bursting dynamics. The frequency of PSCs (and mEPSCs) in experiments decreases with the inhibitory percentage, suggesting a decreasing number of connections per neuron. Accordingly, we assume that the number of excitatory connections per neuron is proportional to the number of excitatory neurons.

Our simulations confirm that the model can qualitatively fit the neuronal dynamics of cultured neurons (Fig. 2*B*). Here, we aim at a quantitative fit that will allow to interpret differences and similarities between the cultures with different E/I ratios. As described in *SI Appendix*, Table S3, most of the parameters of the model are fixed and constrained to lie within the corresponding intervals determined by experiments (ours and in those found in the literature). To avoid overfitting, we fit only the number of inhibitory connections per neuron and the properties of the external drive using Approximate Bayesian Computation (ABC) (23). All other single neuron and network parameters are kept constant. We separately fit networks with E/I ratios corresponding to the various seeded fractions of inhibitory neurons. For extreme 0 and 100% inhibitory networks, we assume 5 and 92% of inhibitory neurons. ABC allows us to approximately solve Bayesian inference problems by minimizing a distance function and returning a joint distribution of the number of inhibitory connections per neurons and external input rate, called posterior distribution. We define the distance function between the model data and the recordings as the mean squared error (MSE) between the vectors of normalized means and CVs of the IBIs. Parameters sampled from this distribution result in a model with dynamics that are similar to bursting in vitro.
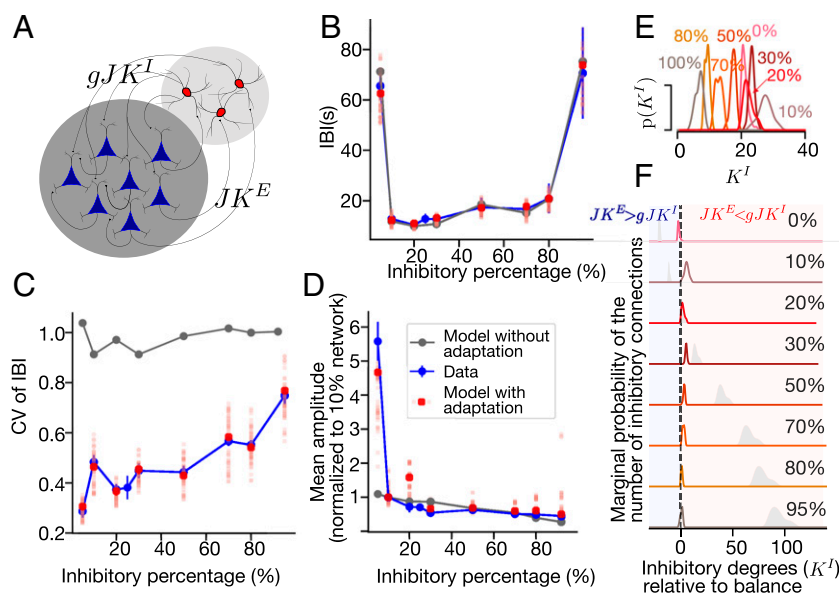

Fig. 5. Network model with adaptive LIF neurons reproduces the main burst features. (*A*) A schematic of the model (see text for details). (*B* and *C*) IBIs (*B*) and CV (*C*) in the model with adaptation (red) and without (gray). The experimental data is shown in blue (error bars, SEM). For the model with adaptation, points (red) show the IBIs in the model with the most probable parameters of an approximated posterior distribution and individual samples are shown in pale red. The model without adaptation cannot reproduce the observed CV, while with adaptation it does. (*D*) Burst amplitudes in cultures (blue) and in the model with adaptation (red, like *B*), normalized by the mean amplitude of the bursts in the 10% inhibitory network. (*E* and *F*) Posterior distributions of the number of inhibitory connections P(KI) obtained by ABC. In *F*, the *x*-axis is shifted such that zero (KI = KE/g) is at balance. The blue regions indicate a part of the parameter space with more excitatory connections than at balance, and red indicates those with more inhibitory connections. They gray shadows show the distributions that would be obtained if the number of inhibitory connections is proportional to the number of inhibitory neurons, taking 20% inhibitory neurons as a reference.

Sukenik et al.
Neuronal circuits overcome imbalance in excitation and inhibition by adjusting connection numbers

PNAS | 5 of 9
https://doi.org/10.1073/pnas.2018459118

After fitting, the network model matches extremely well with the corresponding features of bursting in cultured networks with different inhibitory percentages (Figs. 2B and 5 B–D). With just two individually adjusted parameters, our network accurately fits the important features of the recordings, including nearly constant mean IBIs in networks with 10 to 80% inhibitory percentages and an increase of the mean IBI in networks with extreme inhibitory fractions (Fig. 5B). The model also reproduces the linear increase of the CV of IBIs as a function of inhibitory percentage (Fig. 5C). Surprisingly, the burst amplitudes that are not included in the minimized distance function also match the experimental data (Fig. 5D)

We analyze the posterior distribution of inhibitory connections that leads to good approximations of the bursting features (Fig. 5 E and F). In networks with 10 to 100% inhibitory neurons, the maximum a posteriori estimate of the inhibitory connections is proportional to the number of excitatory connections. In this way, excitatory and inhibitory connections can balance each other in comparison to the naively expected distribution, where the number of connections is proportional to the number of inhibitory neurons (Fig. 5F, gray lines). The posterior distribution of inhibitory connections in networks with 0% inhibitory neurons shifts toward the excitation-dominated region (Fig. 5F, blue region).

We attempt to reduce the complexity of the model by removing the spike-triggered adaptation. A network of LIF neurons without adaptation can exhibit noise-induced population bursts that recapitulate some of the features of bursting in vitro. However, the CV of IBIs in the model without adaptation always stays close to unity, reflecting an exponential distribution of the IBIs (Fig. 5 B and C, gray). Thus, this model fails to capture even basic features of the population bursts in experiments.

Interaction of the E/I Balance and Adaptation. The LIF network with spike-triggered adaptation allows us to effectively describe the network bursting as bistable dynamics driven by the interaction of excitation, inhibition, and adaptation (21, 22). The adaptation current in our model sets the slowest timescale of the IBIs. The inhibitory connectivity can practically be modified in the model

by varying the relative strength of inhibitory synapses, g. When the network does not have inhibition, each burst is terminated only by strong adaptation that counteracts excitation. After that, the adaptation current decays exponentially, and the probability of initiating the next burst gradually increases. Correspondingly, in this regime of activity, the variability of IBIs is small. Adding inhibition to the network allows for shorter IBIs. In this case, both inhibition and adaptation counteract excitation to stop the burst. This results in a much smaller adaptation current at the point of burst termination, increasing the probability of starting the next burst earlier. If the firing rate within the burst is high, the following IBI should be large, allowing the adaptation current to reach sufficiently low values. Altogether, this should result in positive correlations between the burst amplitude and following IBI, which we indeed observe in the experimental data (*SI Appendix*, Fig. S10).

To formalize this idea, we analyze the bursting dynamics, assuming that the spike-triggered adaptation timescale is much slower than the membrane timescale (*SI Appendix*, Table S4). We estimate the stationary firing rate at different fixed levels of adaptation using the current-to-rate transfer function of the white noise–driven LIF neuron and mean-field approximations of the synaptic input (3).

As shown in Fig. 6A, bursts start by bifurcating from a low firing state to the bistable firing regime (squares; left arrows); at this stage, adaptation increases proportionally to the firing rate (upper arrows). This drives the system to eventually transit to the low firing rate state, terminating the burst (circles; right arrows). After that, the adaptation slowly decreases until a new burst can start (bottom arrows). Black lines show stationary firing rates of the network with 20% inhibitory neurons, solved for different adaptation values (solid lines, stable fixed points; dashed lines, unstable fixed points) for two different inhibitory strengths (g = 4, balance condition; g = 3.6, excitation-dominated condition). Pale lines show example trajectories of individual bursts from the network simulation (pink, balanced network; blue, excitation dominated). Larger values of the adaptation at the end of the burst lead to longer IBIs (g = 4 versus g = 3.6). The trajectory of network simulations at the end of the burst do not cross the analytically
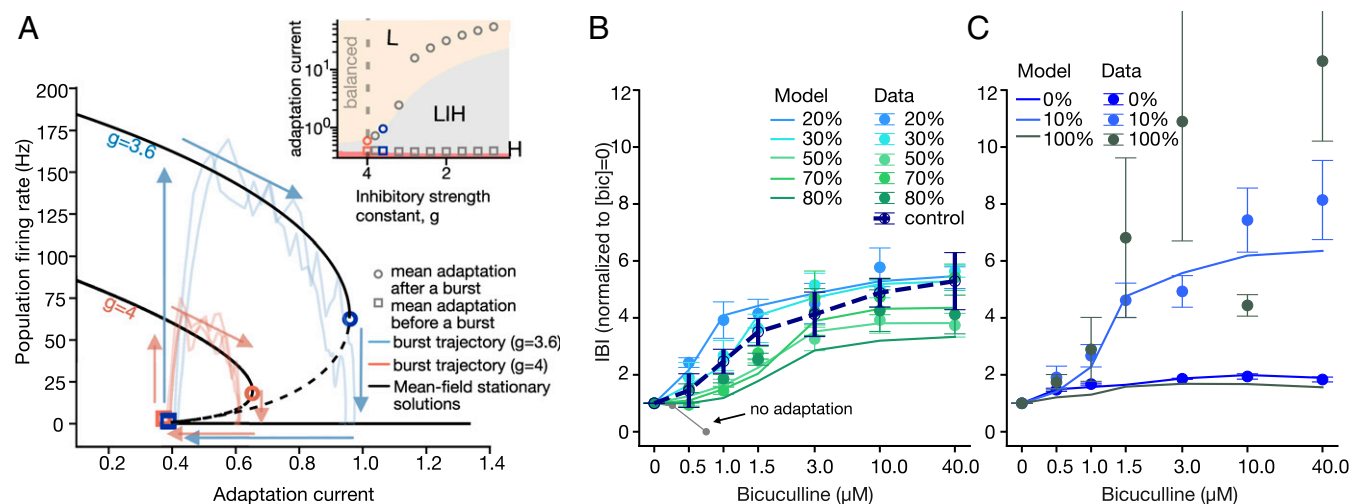

Fig. 6. Blocking of inhibitory synapses reveals the bursting mechanisms. (A) Trajectories in a phase space defined by the population firing rate and spike-frequency adaptation for inhibitory strengths g = 3.6 and g = 4.0 (solid black lines, stable solutions; dashed lines, unstable solutions). At g = 4, the network is in the balance condition; at g = 3.6, it is in the excitation-dominated condition. The pale lines show examples of individual burst trajectories (pink, balanced network; blue, excitation dominated). Larger values of the adaptation at the burst end lead to longer IBIs. (Inset) The size of the bistable region increases with decreasing inhibitory strength. The squares and circles indicate the average adaptation at the beginning and end of simulated bursts. Decreasing the inhibitory strength leads to higher burst amplitudes and longer IBIs. (B) In networks with 20 to 80% of inhibitory neurons, the increase in bicuculline concentration (logarithmic scale) results in longer IBIs—that is, within experimental error, similar to the control cultures. The model (lines) reproduces the experimental results (dots). In contrast, no adaptation model (gray) decreases the IBIs and transitions to a nonbursting dynamic. The IBIs are normalized by the mean at 0 μM bicuculline. (C) Bicuculline application to networks with extreme inhibitory percentages and the corresponding responses of the model.

computed bifurcations (circles) because of inertial effects in stochastic bifurcations (black versus pale blue and pink lines). The inset to Fig. 6A shows that the size of the bistable region increases with decreasing strength of inhibitory synapses.

We thus identify three types of solutions: a fixed point at high firing rate with small adaptation current, a low firing rate fixed point for large adaptation, and a bistable firing rate for intermediate adaptation (Fig. 6 A, Inset; colored areas, small high firing rate regions near x-axis [H], bistable firing [LIH], and low firing [L]). Levels of adaptation at the beginning and end of a burst in the network simulation approximately correspond to analytically computed bifurcations (Fig. 6A). Decreasing the strength of inhibitory synapses gradually increases the size of the bistable region, which corresponds to an increase of the adaptation current at the end of the burst (Fig. 6 A, Inset) and leads to longer IBIs and to larger burst amplitudes.

Inhibition Blockade Probes the Limits of Agreement between Experiment and Model. Our finding, so far, is that networks with all but extreme fractions of inhibitory neurons adapt during development and behave similarly to control cultures. To test what further changes occur under an acute change of synaptic strength, we block inhibitory connections using the synaptic inhibitory blocker, bicuculline (Fig. 6B). All cultures, with different E/I ratios, show a gradual increase of the mean IBI values as a function of inhibitory receptors blockade. The change of IBI in 20 to 80% cultures with saturating amounts of bicuculline ([bicuculline] = 40 µM) is between 3.7 ± 0.8 and 5.6 ± 0.3, and they behave approximately like control cultures (Fig. 6B).

Cultures with almost no inhibition are only slightly sensitive to inhibition blockade in comparison to control (Fig. 6C) and show an increase of 1.8 ± 0.1 in IBI values ($P = 0.0181$), whereas cultures that are mainly inhibitory are highly sensitive to bicuculline (11 ± 6 times increase of IBIs already at [bicuculline] = 3 µM) and show a high variability of responses. Some of the 10% inhibitory cultures exhibit a unique behavior, with a sharp increase in IBI values ranging between 7 to 16 times at [bicuculline] = 40 µM.

To repeat these experiments in silico, we gradually decrease the strength of inhibitory connections in models fitted to the experimental data without application of bicuculline. We approximate the decrease of the inhibitory strength by the fraction of inhibitory receptors blocked $1/\left(1 + \frac{[\text{bicuculline}]}{K_d}\right)$, where $K_d = 3$ µM (20). Networks with adaptation respond by increasing the mean IBI, closely matching the experimental results (Fig. 6 B and C, note that we did not refit the networks to match the bicuculline responses). In contrast, the networks without adaptation decrease the mean IBIs (Fig. 6B, gray).

Next, we quantify how deviations from balance affect the response of the model network to bicuculline, where deviation 0 means that the excitatory and inhibitory connections are at balance: $JK^E = gJK^I$. To this end, we investigate the set of networks parametrized by the deviation from balance. We measure the MSE between the bicuculline responses recorded in vitro and the responses of networks. In 20 to 80% networks, the best matching responses came from the models with nearly balanced E/I connections (*SI Appendix*, Fig. S9).

For extreme values of the E/I ratio, the network shows most interesting behavior, and from 10% inhibition and below, a transition occurs where IBIs show an increase. According to the model, this indicates that the network begins to fail in attaining structural E/I balance at 10%. In 0 and 10%, the best parameters are found to be in the excitation-dominated region and in the inhibition-dominated region, respectively. At the other extreme of 100% inhibitory neurons, the responses are highly variable, deviate significantly from the model, and cannot be predicted by it. The network model with 100% inhibitory neurons fails to show a response to bicuculline with the magnitude observed in vitro (Fig. 6C). Altogether, for all but extreme fractions, the networks faithfully reproduce the responses to all intermediate bicuculline concentrations, with the best matching parameters either at the maximum a posteriori estimate or situated slightly closer to the balance point.

Discussion

E/I balance is a state attractor of neuronal networks. Our first and main finding is that a living neuronal network will flow toward a state attractor characterized by an E/I balance. This tendency for network behavior occurs for a wide variety of cellular E/I fractions, ranging from ∼10 to 80% of inhibitory neurons, where the networks adapt and develop stable, spontaneous network activity. The main mechanism that we identify for this stability is the maintenance of balanced E/I connectivity.

The theoretical role of E/I balance in network dynamics and function has been discussed in earlier works (24). The flow toward an attractor with balanced dynamics was previously observed to be the typical response of cultured neuronal networks after a prolonged perturbation (25). Also, many experimental results displayed a dynamic E/I balance in a wide range of neuronal circuits, including the neocortex, hippocampus, and spinal cord (1, 2, 8, 16). Furthermore, several studies found that the dynamic balance of excitatory and inhibitory currents relies on balanced E/I connectivity (8, 9). Most of the networks that have balanced E/I dynamics also have a tightly preserved ratio of excitatory and inhibitory neurons (5).

Our results are in agreement with earlier studies on the development of single-cell input connectivity (8). Liu (8) reported that the ratio of E/I connections on a dendrite of a single neuron is fixed and that E/I currents balance each other already at the single-dendrite level. They also proposed that the balance is controlled by a compensatory push–pull mechanism that is established by chronically blocking and activating excitatory and inhibitory receptors. Our study indicates that cultured networks tend to maintain the balanced E/I connectivity even under the challenge of extreme and long-term changes of cellular composition.

Structural E/I balance may be regulated by changes in connectivity. We have seen that the control over structural E/I balance in the dissociated hippocampal cultures is achieved by pruning the number of connections in networks that have an increased number of inhibitory cells. The frequency of both PSCs and mEPSCs decreases with inhibitory percentage; however, their size does not, suggesting that the number of connections decreases in proportionality to the E/I ratio.

The frequency of PSCs is most probably dominated by excitatory inputs, and therefore we assume that it decreases in a direct proportion to the number of excitatory cells. Thus, the network model is constructed under the assumption that the number of excitatory inputs decreases linearly with the fraction of excitatory neurons. The fitted model suggests that the number of inhibitory connections dramatically changes in order to maintain balanced E/I connectivity and to compensate for the perturbation of the cellular composition.

These differences underlie practically all of the changes in spontaneous network activity that we observe. For instance, a dramatic decrease in the number of connections in the network that contains almost only inhibitory neurons leads to the prolongation of IBIs. We have explored this result by building a network model under the assumption that the number of connections decreases in networks with a higher fraction of inhibitory neurons while the ratio of excitatory and inhibitory connections remains fixed. Although we use a very simplified single-neuron model, we could fit the temporal aspects of the bursting dynamics extremely well.

Our results complement earlier studies of systematic manipulation of the network structure (9, 26, 27). Wilson et al. (26) studied the effects of the network size on the connectivity and

Sukenik et al.
Neuronal circuits overcome imbalance in excitation and inhibition by adjusting connection numbers

PNAS | 7 of 9
https://doi.org/10.1073/pnas.2018459118

dynamics. They show that the firing rates of neurons were preserved across networks of different sizes even though the number of neurons and synapses increased. The result was due to the fact that the number of excitatory inputs was compensated by synaptic strength. Interestingly, they showed that amplitudes of mEPSCs are larger in the smaller cultures while, in our case, we do not see substantial differences in mEPSC amplitudes. What is most striking in our networks is changes in mEPSC frequencies, which does not change in their networks. Ivenshitz & Segal (27) showed how changing the density of hippocampal cultures affects the spontaneous activity and linked these changes to the differences in synaptic organization. In their study, the average duration of IBIs, as well as the burst amplitudes, increases in sparser networks. This change is governed by an increase in the amplitudes of the PSCs along with a decrease in the number of connections, which is opposite to the synaptic changes that we have found.

Barral and Reyes (9) extended this result to cortical cultures of various densities. They showed that the synaptic strength changes as the inverse of the square root of the number of connections while preserving the balance between incoming excitatory and inhibitory connections as predicted by theory (24). In contrast, our results indicate that long-term changes in the cellular E/I ratio radically change the input connectivity rather than the synaptic strength.

Inhibition controls variability. We have found that, while the number of inhibitory neurons does not affect the average spontaneous activity in the cultured network, it strongly affects its variability (i.e., the higher order statistics of the bursts). The CV of IBIs grows linearly with the number of inhibitory neurons in the culture. Thus, networks with the highest numbers of inhibitory cells and only a small fraction of excitatory cells have the highest CV, which approaches unity. The bursting dynamics in these networks thus resemble a Poisson process. This is possibly a consequence of a smaller number of connections in networks with high numbers of inhibitory neurons, which decorrelates the input into neurons and randomizes bursting events (28). This could obviously have an impact on the reliability of neuronal circuitry.

Inhibition can also directly influence the bursting variability, as indicated by several theoretical and experimental studies (4, 29). An increase in the inhibitory synaptic strength or number of connections makes inputs less synchronized, which consequently decreases the burst amplitude and increases the variability of IBIs.

Conclusion

In summary, we present a system where the impact of the cellular E/I composition on neuronal network organization and dynamics can be quantitatively evaluated. Cultured neuronal networks exhibit stable and balanced dynamics within a wide range of externally imposed initial cellular E/I ratio. We present evidence supporting the idea that adjustment of the number of input connections to each neuron in the network is the dominant mechanism for maintaining the E/I balance. We explain the collective dynamics of cultured neuronal networks with varying E/I ratios using a minimal theoretical model. The observed dynamics are described in terms of an interaction between inhibition and adaptation. The model reliably reproduces the experimental observations when inhibitory and excitatory connections are balanced.

Inhibition is a basic component of neuronal networks, and our understanding of its role in network dynamics and function is constantly being extended. Early studies suggested that inhibition is a simple negative feedback mechanism to avoid runaway excitation (13). Further studies established the crucial role of inhibition in the dynamical repertoire (3), response properties, and coding capacity (24, 30). More recently, Mongillo et al. (31) theoretically showed that inhibitory connectivity increases the memory storage capacity. Our experimental platform allows us to precisely control the E/I network architecture and opens possibilities for detailed studies of E/I circuitry.

Overall, these findings signify that, when an externally imposed alteration of the E/I ratio is given in an early stage of development, the system adapts and overcomes it to maintain stable and balanced dynamics. Since the network we engineer is randomly connected and its architecture is very different from that of networks in the brain, our finding that bursts are robustly controlled must be translated into a relevant conclusion for brain circuits. This promises to be a future challenge.

Materials and Methods

Labeled dissociated neurons from a mouse hippocampus are sorted with FACS to manipulate the number of excitatory and inhibitory cells. Whole-network spontaneous activity is recorded with a Fluo-4 calcium indicator. PSC and mPSC are recorded using the patch-clamp method across networks with different E/I ratios. The network of excitatory and inhibitory LIF neurons is fitted to the experimental data using ABC. We fit the number of inhibitory connections and the external input rate while keeping the other parameters constant at the physiologically realistic values. Please refer to *SI Appendix, SI Methods* for the detailed description and further information about the data analysis and statistics.

Data Availability. All data and codes used for data analysis and network simulations will be available upon publication. Code, calcium imaging network traces, and single-cell patch-clamp measurements data have been deposited in Figshare, figshare.com (https://figshare.com/projects/Neuronal_circuits_overcome_imbalance_in_excitation_and_inhibition_by_adjusting_connection_numbers/88586). The code for network simulations is also available at GitHub, https://github.com/LevinaLab/PNAS-2021.

1. J. S. Isaacson, M. Scanziani, How inhibition shapes cortical activity. *Neuron* **72**, 231–243 (2011).

2. M. Okun, I. Lampl, Instantaneous correlation of excitation and inhibition during ongoing and sensory-evoked activities. *Nat. Neurosci.* **11**, 535–537 (2008).

3. N. Brunel, Dynamics of sparsely connected networks of excitatory and inhibitory spiking neurons. *J. Comput. Neurosci.* **8**, 183–208 (2000).

4. G. Gigante, G. Deco, S. Marom, P. Del Giudice, Network events on multiple space and time scales in cultured neural networks and in a stochastic rate model. *PLOS Comput. Biol.* **11**, e1004547 (2015).

5. S. Sahara, Y. Yanagawa, D. D. M. O'Leary, C. F. Stevens, The fraction of cortical GABAergic neurons is constant from near the start of cortical neurogenesis to adulthood. *J. Neurosci.* **32**, 4755–4761 (2012).

6. J. Chapeton, T. Fares, D. LaSota, A. Stepanyants, Efficient associative memory storage in cortical circuits of inhibitory and excitatory neurons. *Proc. Natl. Acad. Sci. U.S.A.* **109**, E3614–E3622 (2012).

7. V. Capano, H. J. Herrmann, L. de Arcangelis, Optimal percentage of inhibitory synapses in multi-task learning. *Sci. Rep.* **5**, 9895 (2015).

8. G. Liu, Local structural balance and functional interaction of excitatory and inhibitory synapses in hippocampal dendrites. *Nat. Neurosci.* **7**, 373–379 (2004).

9. J. Barral, A. D Reyes, Synaptic scaling rule preserves excitatory-inhibitory balance and salient neuronal network dynamics. *Nat. Neurosci.* **19**, 1690–1696 (2016).

10. D. M. Kullmann, Interneuron networks in the hippocampus. *Curr. Opin. Neurobiol.* **21**, 709–716 (2011).

11. D. Eytan, S. Marom, Dynamics and effective topology underlying synchronization in networks of cortical neurons. *J. Neurosci.* **26**, 8465–8476 (2006).

12. O. Feinerman, M. Segal, E. Moses, Signal propagation along unidimensional neuronal networks. *J. Neurophysiol.* **94**, 3406–3416 (2005).

13. M. A. Dichter, G. F. Ayala, Cellular mechanisms of epilepsy: A status report. *Science* **237**, 157–164 (1987).

14. A. H. Taub, Y. Katz, I. Lampl, Cortical balance of excitation and inhibition is regulated by the rate of synaptic activity. *J. Neurosci.* **33**, 14359–14368 (2013).

15. O. Yizhar *et al.*, Neocortical excitation/inhibition balance in information processing and social dysfunction. *Nature* **477**, 171–178 (2011).

16. R. W. Berg, A. Alaburda, J. Hounsgaard, Balanced inhibition and excitation drive spike activity in spinal half-centers. *Science* **315**, 390–393 (2007).

17. E. Tibau, M. Valencia, J. Soriano, Identification of neuronal network properties from the spectral analysis of calcium imaging signals in neuronal cultures. *Front. Neural Circuits* **7**, 199 (2013).

18. J. Soriano, M. Rodríguez Martínez, T. Tlusty, E. Moses, Development of input connections in neural cultures. *Proc. Natl. Acad. Sci. U.S.A.* **105**, 13758–13763 (2008).

19. M. Segal, V. Greenberger, E. Korkotian, Formation of dendritic spines in cultured striatal neurons depends on excitatory afferent activity. *Eur. J. Neurosci.* **17**, 2573–2585 (2003).

20. S. Jacobi, J. Soriano, M. Segal, E. Moses, BDNF and NT-3 increase excitatory input connectivity in rat hippocampal cultures. *Eur. J. Neurosci.* **30**, 998–1010 (2009).

21. M. Giugliano, P. Darbon, M. Arsiero, H. R. Lüscher, J. Streit, Single-neuron discharge properties and network activity in dissociated cultures of neocortex. *J. Neurophysiol.* **92**, 977–996 (2004).

22. E. M. Tartaglia, N. Brunel, Bistability and up/down state alternations in inhibition-dominated randomly connected networks of LIF neurons. *Sci. Rep.* **7**, 11916 (2017).

23. M. Sunnåker *et al*., Approximate Bayesian computation. *PLoS Comput. Biol.* **9**, e1002803 (2013).

24. C. van Vreeswijk, H. Sompolinsky, Chaos in neuronal networks with balanced excitatory and inhibitory activity. *Science* **274**, 1724–1726 (1996).

25. M. Kaufman, S. Reinartz, N. E. Ziv, Adaptation to prolonged neuromodulation in cortical cultures: An invariable return to network synchrony. *BMC Biol.* **12**, 83 (2014).

26. N. R. Wilson, M. T. Ty, D. E. Ingber, M. Sur, G. Liu, Synaptic reorganization in scaled networks of controlled size. *J. Neurosci.* **27**, 13581–13589 (2007).

27. M. Ivenshitz, M. Segal, Neuronal density determines network connectivity and spontaneous activity in cultured hippocampus. *J. Neurophysiol.* **104**, 1052–1060 (2010).

28. D. Lonardoni *et al*., Recurrently connected and localized neuronal communities initiate coordinated spontaneous activity in neuronal networks. *PLoS Comput. Biol.* **13**, e1005672 (2017).

29. M. V. Sanchez-Vives *et al*., Inhibitory modulation of cortical up states. *J. Neurophysiol.* **104**, 1314–1324 (2010).

30. S. Denève, C. K. Machens, Efficient codes and balanced networks. *Nat. Neurosci.* **19**, 375–382 (2016).

31. G. Mongillo, S. Rumpel, Y. Loewenstein, Inhibitory connectivity defines the realm of excitatory plasticity. *Nat. Neurosci.* **21**, 1463–1470 (2018).

NEUROSCIENCE

BIOPHYSICS AND COMPUTATIONAL BIOLOGY